# INDOCHINITE TEKTITE SUBORBITAL ASSESSMENT.

T. H. S. HARRIS[1] [1]GE Astro Space Div., Lockheed Martin, Boeing Helicopter, retired (thsharris1@icloud.com, Brooklyn NY)

**Introduction:** Tektites represent shocked and melted distal ejecta of terrestrial cosmic impacts, composed primarily of silicate sediments outgassed and quenched to glassy solid while still in vacuum. Their formative and propulsive processes are not fully understood, including likely volatile jetting entrainment among many other topics. The 789ka Australasian tektite (AAT) case with yet-unlocated parent impact structure has uniquely large partitioned Kinetic Energy (KE) scale based on melt mass and strewnfield size. Suborbital AAT transport assessment offers insight for the AAT source structure search.

**Discussion:** 1960s NASA ablation researchers resolved the heat transfer equation for spaceflight's hypervelocity atmospheric entry regime. Calibrating the equation's coefficients by reproducing naturally occurring ablated tektite morphology provides the *ablation regime diagram* concept of Fig. 1 from [1], where effects of speed, flight path angle from horizontal and dynamic pressure (not labelled) provide ablation sub-regime bounds for 'perfect button' tektite specimens, labeled P.B. 1, P.B. 4, etc.

In Fig. 1, angle-labeled arcs represent the central flight angle $\theta$ and flight path angle $\boldsymbol{\gamma_i}$ (= elevation EL) per the right-side coordinate definition, with trajectory direction arrows instead of ***A*** and ***B*** at respective launch and fall points. Smaller values of $\theta$ in Fig. 1 require less speed and are highly dependent on reentry flight path angle $\gamma_i$, which equates to launch elevation 'EL' via suborbital symmetry. NASA'S 1960s tektite transport assessment used the simplified 2-body model available in the public domain at the time. Uses of that period are depicted in Figure 2. Derived in non-rotating 2-dimensional space, it *did not* account for Earth's rotation. Dobrovolskis (1981) [2] provides a generalized 3-D ***A***-to-***B*** suborbital ejecta transport model with planetary rotation per Figure 3.

**Figure 1.** *A) 'Perfect button' tektite 3-view, and B) 1960s NASA research [1] (Fig. 23, p65) ablation regime diagram with coordinate definition at lower right, central flight angle $\theta$ and flight path angle $\gamma_i$. The non-rotating model fails dynamically: duration-induced westerly fall point shift blows up as speed increases to significant fractions of Earth's escape KE.*

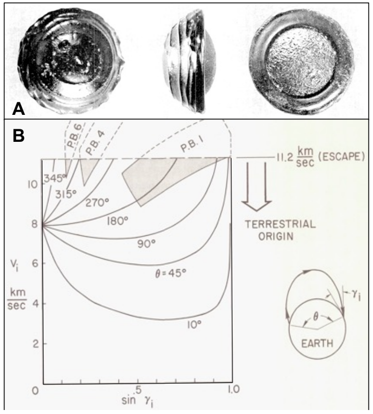

**Figure 2.** *Various 2-D treatments of the simplified two-body model available to the 1960s civil sector do not account for Earth's rotation during tektite loft.*

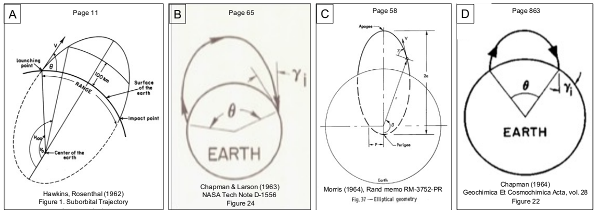

Hawkins, Rosenthal (1962) Figure 1. Suborbital Trajectory

Chapman & Larson (1963) NASA Tech Note D-1556 Figure 24

Morris (1964), Rand memo RM-3752-PR Fig. 37 — Elliptical geometry

Chapman (1964) Geochimica Et Cosmochimica Acta, vol. 28 Figure 22

**Figure 3.** *Derived in 3-space, Dobrovolskis (1981) [2] treats the rotation of the planet as indicated by the $\omega \cdot T$ term of spherical trigonometry setup (right), where $\omega$ is angular rate and $T$ is nondimensionalized time, central flight angle in orbit plane is $\Delta$ instead of $\theta$, and $\theta$ is launch/fall elevation angle from local vertical.*

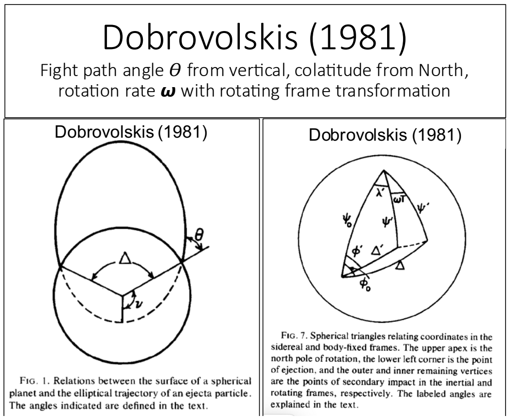

Dobrovolskis (1981)

Fight path angle $\theta$ from vertical, colatitude from North, rotation rate $\boldsymbol{\omega}$ with rotating frame transformation

Dobrovolskis (1981)

FIG. 1. Relations between the surface of a spherical planet and the elliptical trajectory of an ejecta particle. The angles indicated are defined in the text.

Dobrovolskis (1981)

FIG. 7. Spherical triangles relating coordinates in the sidereal and body-fixed frames. The upper apex is the north pole of rotation, the lower left corner is the point of ejection, and the outer and inner remaining vertices are the points of secondary impact in the inertial and rotating frames, respectively. The labeled angles are explained in the text.

The 1960s suborbital ballistic treatments did not elaborate on 2$^{nd}$-way trajectories that exist for the ***A***-to-***B*** suborbital problem, later addressed in [3]. At higher fractions of Earth's escape KE, long-way or 2$^{nd}$-way trajectories (central flight angle 'θ' or 'Δ' > 180°) are more likely for launch elevation < 45° from horizontal, while more steeply vertical launch angles can't reach antipodally without aid of planetary rotation, per [2].

Loft duration as a function of launch angles and speed, illustrated in the non-rotating frame by [4] of Fig. 4A is expanded in Fig 4B to compare Earth's worst case rotational effect of equatorial East or West launch and low elevation. Horizontal launch is the left side and vertical launch the right in the Figure 4 diagrams. Higher KE extended loft pushes the fall point West on rotating Earth beneath the inertially fixed orbit plane. Harris (2022) [5] provides suborbital analysis shareware to solve for the set of all ***A***-to-***B*** suborbital solutions, from minimum- to minimum + 26 hours loft.

**Figure 4.** *1960s [4] 2-D model in frame A at left is expanded for Earth's rotational effects in frame B at right. 10 km/s minimum speed of high-ablation Victoria-ite button tektites per [1] implying ~3.5 to 12 hours loft duration and interhemispheric transport.*

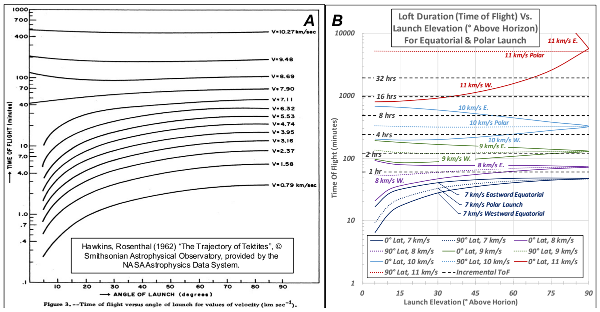

**Figure 5.** *Atmospheric reentry regime diagram improved from [1] of Fig. 1 shows 1st-way or short-way (blue) & 2nd-way or long-way (green)* ***A*-to-*B*** *suborbital solution sets from Lake Huron N. America per [5,6] to Huai Om Northeast Thailand where large areas of impact clastics were rapidly overlain by AAT-bearing laterite and then meters of sand fining upward [7].*

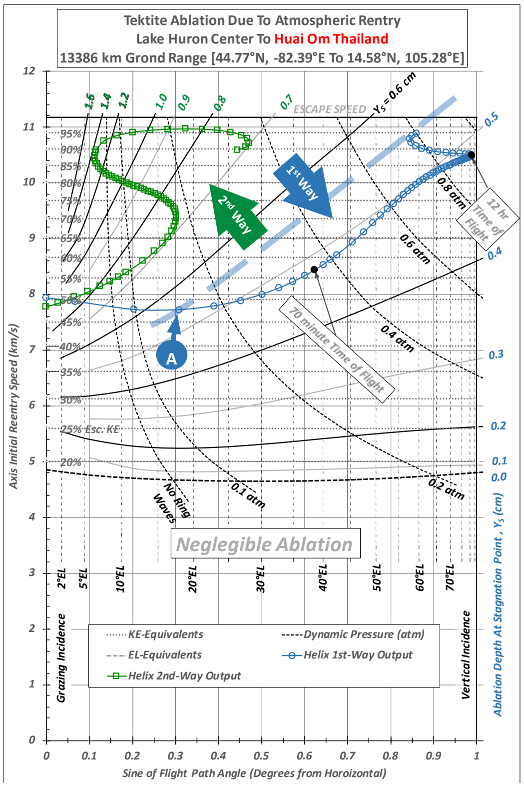

The 1st- and 2nd-way ***A***-to-***B*** suborbital solution sets are shown in Fig. 5, with Lake Huron in N. America considered as an AAT source region per [5,6] and fall point Huai Om, northeast Thailand per [7].

Both 1st and 2nd ***A***-to-***B*** suborbital solution sets convolute with increasing KE due to Earth's spin (Fig. 5, top). Green 2nd-way solutions hug the high-ablation upper left portion of the diagram (0.7 to 1.4 cm ablation contours), *unlike* the indochinite tektite sample population. Blue 1st-way or short-way solution family follows the 0.5 cm ablation contour as launch EL as KE increase per the blue arrow in Fig. 5. Ablation-limiting is *inherent* in 1st-way or short-way solutions for this ***A***-to-***B*** suborbital pair, remaining relatively low from ~8.4 to 10.5 km/s (black dots on blue curve) due to heating impulse timescale compression of steep reentry angles.

Tumbling upon reentry can also reduce or eliminate ablated mass loss. Indochinite fragment forms exhibit feature sets consistent with high-voltage arcing disruption from cold state (fracture) overprinted by visco-plastic thermal-momentum features (uniaxial extension/compression, blast-contortion, planar marginal beveling, concentric cardioid lobate surface striae, etc.). Irregular shapes and their likely non-zero tumble rates help explain reduced fragment-form indochinite ablation up to 10.5 km/s reentry speed.

**Summary:** Steep descent angles and tumbling, irregular form factors limit reentry ablation, while antipodal ground range remains possible or probable at the high indicated KE of the AAT. Less reentry ablation of Indochinite AAT compared to their Australite or Central Indian Ocean ablated button kin is explained by a more vertical 1st-way reentry angle from a source substantially up-spin or East of S.E. Asia at mid or high northern latitude. Ejecta melt speeds reaching above 10 km/s (> 80% escape KE) [1] and the large AAT strewnfield area with interwoven geochemical subfamilies indicate interhemispheric suborbital transport, likely combined as both 1st- & 2nd-way.

Questions remain regarding tektite-bearing laterite of Huai Om, northeast Thailand [7]: how does significant laterization of an entire regional surface happen in a few hours between impact surge deposit, tektite fall and subsequent blanketing by upward-fining sand? (Where did the hot moisture come from, how was it heated/forced, involved in partitioning, etc.?)

**References:** [1] Chapman, Larson (1963) *NASA TN D-1556*. [2] Dobrovolskis (1981) *Icarus 47*, 203-219. [3] Bate, Mueller, White (1971) *Fundamentals of Astrodynamics*. [4] Hawkins, Rosenthal (1962) *The Trajectory of Tektites*, Smithsonian Astrophysical Observatory. [5] Harris (2022), *GSA Books vol. 553* ch. 23. [6] Davias, Harris (2022), *GSA Books vol. 553* ch. 24. [7] Tada et al. (2022) *Meteoritics & Planet. Sci., 57*, Nr 10, 1879–1901.